



Contents lists available at ScienceDirect

## Chemical Physics Letters

journal homepage: [www.elsevier.com/locate/cplett](http://www.elsevier.com/locate/cplett)

# Realization of the bond order wave (BOW) phase of extended Hubbard models in Rb–TCNQ(II)

T.M. McQueen<sup>a</sup>, D.M. Ho<sup>b</sup>, C. Jiménez Cahua<sup>a</sup>, R.J. Cava<sup>a</sup>, R.A. Pascal Jr.<sup>a</sup>, Z.G. Soos<sup>a,\*</sup>

<sup>a</sup> Department of Chemistry, Princeton University, Princeton, NJ 08544, United States

<sup>b</sup> Department of Chemistry and Chemical Biology, Harvard University, Cambridge, MA 02138, United States

## ARTICLE INFO

## Article history:

Received 12 February 2009

In final form 29 April 2009

Available online xxx

## ABSTRACT

Rb–TCNQ(II) is shown to be a realization of the BOW phase of half-filled extended Hubbard models. The BOW phase has a regular array of sites with inversion ( $C_i$ ) symmetry, a finite magnetic gap  $E_m$  and broken electronic  $C_i$  symmetry. The phase is conditionally stable against dimerization for linear electron–phonon (e–ph) coupling. At 100 K, Rb–TCNQ(II) crystals have regular TCNQ<sup>−</sup> stacks at  $C_i$  centers, negligible spin susceptibility that indicates finite  $E_m$ , and infrared (ir) spectra that indicate broken  $C_i$  symmetry. The 100 and 295 K crystal structures rule out a dimerization transition around 220 K that had previously been inferred from magnetic and ir data.

© 2009 Elsevier B.V. All rights reserved.

## 1. Introduction

The half-filled extended Hubbard model (EHM) in one dimension (1D) illustrates competition among electron transfer  $t$ , on-site repulsion  $U > 0$  and nearest-neighbor interactions  $V > 0$ . Large  $U$  gives a ground state (gs) with one electron per site while large  $V > V_c$  gives a charge density wave (CDW) with alternately empty and doubly occupied sites. Nakamura [1] proposed that the EHM has a bond order wave (BOW) phase at 0 K for  $V$  slightly less than  $V_c \sim U/2$  that marks the CDW transition and large enough  $t/U$  to have a continuous CDW transition. The BOW phase has long-range order, a finite magnetic gap  $E_m$  and broken electronic inversion ( $C_i$ ) symmetry. A new phase in a familiar solid-state model attracted much theoretical attention [2–4], initially to debate its existence and later to delineate its narrow range from  $V_s(U)$  to  $V_c(U)$  for  $U < U'$ , the critical point at which the CDW transition becomes discontinuous. BOW studies [1–4] of the EHM refer to the electronic gs of a rigid 1D regular (equally spaced) array. The possibility of physical realizations has not been raised.

We consider, in this Letter, a physical realization of a BOW phase, and will start with several general requirements. First, Coulomb interactions are more realistic than a nearest-neighbor  $V$ . We recently showed that Coulomb interactions lead to a wider BOW phase near the CDW boundary [5]. Second, the system must be near the CDW boundary. This requirement depends on 3D electrostatic (Madelung) energies in ionic crystals, and is met by 1:1 alkali–TCNQ (tetracyanoquinodimethane) salts [6]. Third, 1D systems such as conductors, conjugated polymers, charge-transfer (CT) salts or spin chains are subject to a Peierls instability and

dimerization in the half-filled case. The stability of a BOW phase with linear electron–phonon (e–ph) coupling is considered in Section 2. The BOW phase is poorly characterized theoretically aside from finite  $E_m$  and broken electronic  $C_i$  symmetry in a structure with  $C_i$  symmetry at sites. These signatures for the existence of a BOW phase follow from symmetry rather than from choices of  $t$ ,  $U$  or other parameters.

Hubbard models are broadly applicable to correlated solid-state systems, including organic salts of strong  $\pi$ -electron donors (D) or acceptors (A) [7–9]. Planar D and/or A often crystallize in face-to-face stacks that point to 1D electronic structure. A = TCNQ forms A<sup>−</sup> stacks of planar radical anions in alkali–TCNQ salts. A 1:1 stoichiometry results in a half-filled band based on the LUMO, with  $t \sim 0.1$ – $0.3$  eV. Vegter and Kommandeur [10] have summarized the identification and characterization of dimerization transitions around  $T_d \sim 300$  K in 1:1 alkali–TCNQ salts. Endres [11] has reviewed metal–TCNQ crystal structures and overlap patterns. Na [12,13] and K–TCNQ [14] structures are known both above and below  $T_d$ ; there are three polymorphs [15–17] of Rb–TCNQ. The compound studied here, Rb–TCNQ(II), has regular stacks [16] at 300 K and a reported [10,18]  $T_d \sim 220$  K. As reviewed by Bozio and Pecile [19], vibrational spectroscopy is widely applicable to quasi-1D organic solids and depends sensitively on  $C_i$  symmetry. Dimerization was the only recognized way to break  $C_i$  symmetry prior to Nakamura's identification of a BOW phase [1].

We report the 100 and 295 K structures of Rb–TCNQ(II) in Section 3. Quite unexpectedly, the  $P1$  structure at 295 K is retained at 100 K, thereby excluding a transition in this range. Previous magnetic [10] and infrared (ir) [18] data are consistent with our samples. Negligible spin susceptibility below 150 K indicates finite  $E_m$ . The appearance of totally symmetric (ts) molecular vibrations in ir spectra, polarized along the stack, indicates broken  $C_i$  symmetry

\* Corresponding author. Fax: +1 609 258 6746.

E-mail address: [soos@princeton.edu](mailto:soos@princeton.edu) (Z.G. Soos).

and is well understood [19] in TCNQ salts with *dimerized* stacks. We find Rb–TCNQ(II) to have a center of inversion by single crystal X-ray diffraction at 100 K, finite  $E_m$  from magnetic susceptibility and broken electronic  $C_i$  symmetry according to ir. These observations are evidence that Rb–TCNQ(II) is a realization of a BOW phase. We briefly mention other alkali–TCNQ data that can be understood qualitatively in terms of a BOW phase.

## 2. BOW phase and dimerization

Each regular TCNQ<sup>−</sup> stack corresponds to a half-filled 1D Hubbard model  $H_0$  with spin-independent interactions between ions. Such models have translational, electron–hole (e–h), and  $C_i$  symmetry. Interest in polyacetylene [20] has motivated extensive studies of Peierls systems. The Su–Schrieffer–Heeger (SSH) model [21] is the generic case: a tight-binding band with  $-t(1 \pm \delta)$ , a harmonic lattice with potential energy  $\kappa u^2/2$  for displacement  $\pm u$  and linear e–ph coupling  $\alpha = (dt/du)$ . Linear coupling is retained in generalizations that entail approximations and include e–e interactions, spin chains, CT salts, continuum models, quantum fluctuations, 3D interactions, molecular vibrations or realistic force fields. We consider unique aspects of a BOW phase and the implications of the 100 K structure.

The electronic  $H$  with gs energy  $\varepsilon_0(\delta)$  per site and  $t = 1$  is

$$H(\delta) = H_0 - \delta H_d \equiv H_0 - \sum_{r\sigma} \delta(-1)^r (a_{r\sigma}^\dagger a_{r+1\sigma} + hc). \quad (1)$$

The lattice is harmonic in  $u$ , and hence in  $\delta = \alpha u/t$ , with inverse stiffness  $\varepsilon_d = \alpha^2/\kappa$  for force constant  $\kappa$ . The total energy per site in the adiabatic approximation is

$$\varepsilon_T(\delta) = \varepsilon_0(\delta) + \delta^2/2\varepsilon_d. \quad (2)$$

A minimum at  $\delta \neq 0$  implies a dimerized gs, and dimerization persists up to some  $T = T_p$ . The Peierls instability of the BOW phase of the EHM with SSH parameters has been studied by Sengupta et al. [22] using Monte Carlo simulations and no adiabatic approximation. They find dimerization at 0 K to be conditional on  $\alpha > \alpha_c$ . We note that Rb–TCNQ(II) has ring-over-bond (tilted) stacks [11] while the Na and K stacking is ring-over-ring (eclipsed) with nearly twice as large [23]  $t$ . Since  $t(u) = t(0)\exp(-\gamma u)$  implies that  $\alpha$  is proportional to  $t$ , e–ph coupling is clearly weaker in Rb(II). Data at lower  $T$  is needed to distinguish between a system with  $\alpha < \alpha_c$  and one with lower  $T_p$ .

In the following, we retain the adiabatic approximation, Eq. (2), and suppose  $H_0$  to have a BOW phase. We label to the gs, degenerate at  $\delta = 0$ , as  $|\psi(B, \delta)\rangle$  and  $|\psi(-B, \delta)\rangle$ , with

$$B \equiv p_+ - p_- = \langle \psi(B, 0) | H_d | \psi(B, 0) \rangle / N. \quad (3)$$

As Eq. (1) is written,  $|\psi(B, 0)\rangle$  has larger bond order  $p_+$  between sites  $2r, 2r+1$  and smaller  $p_-$  between sites  $2r-1, 2r$ . The bond orders of  $|\psi(-B, 0)\rangle$  are reversed. The degeneracy is lifted for  $\delta \neq 0$ :  $|\psi(B, \delta)\rangle$  has lower energy for  $\delta > 0$  and  $|\psi(-B, \delta)\rangle$  for  $\delta < 0$ . To second order in  $\delta$ , the Taylor expansion of  $\varepsilon_T$  is

$$\varepsilon_T(\delta) = \varepsilon_0(0) - B|\delta| + \frac{\delta^2(1 - \varepsilon_d\chi_d)}{2\varepsilon_d}. \quad (4)$$

The linear term is BOW specific. The quadratic term contains an electronic force constant [24],

$$\chi_d = \frac{2}{N} \sum_R |\langle R | H_d | 0 \rangle|^2 / (E_R - E_0). \quad (5)$$

The sum is over the excited states  $|R\rangle$  of  $H_0$  with excitation energy  $E_R - E_0$ . The relevant  $|R\rangle$  are singlets with the same e–h symmetry as the gs [24]. Infinite regular stacks have divergent  $\chi_d$  in the band limit, in Hubbard models with  $U > 0$  or in spin-1/2 Heisenberg

chains; those models are unstable to dimerization. Since two triplets can form a singlet  $|R\rangle$ , the spectrum in Eq. (5) has an energy gap and  $\chi_d$  is finite due to finite  $E_m$ . The quadratic term in  $\varepsilon_T$  is positive for  $\varepsilon_d\chi_d < 1$ , the case considered below that is made possible by finite  $\chi_d$ . Higher-order terms are required in Eq. (4) when  $\varepsilon_d\chi_d > 1$ .

With  $\varepsilon_d\chi_d < 1$  by hypothesis, it is elementary to minimize  $\varepsilon_T$ . The *adiabatic* potential for  $|\psi(B, \delta)\rangle$  is a displaced harmonic oscillator centered at

$$\delta(B) = B\varepsilon_d' \equiv \frac{B\varepsilon_d}{(1 - \varepsilon_d\chi_d)}. \quad (6)$$

The displacement for  $|\psi(-B, \delta)\rangle$  is  $\delta(-B) = -\delta(B)$ , and the energy is lowered by  $B^2\varepsilon_d'/2$ . The *adiabatic* potential in Eq. (4) is wider and not harmonic, however, since  $\delta > 0$  calls for the potential of  $|\psi(B, \delta)\rangle$  and  $\delta < 0$  for that of  $|\psi(-B, \delta)\rangle$ . We consider an oscillator centered at  $\delta = 0$  with potential  $\delta^2/2\varepsilon_d'$  and compute first-order corrections for  $-B|\delta|$ . The regular lattice is stabilized by more than  $B^2\varepsilon_d'/2$  provided that

$$\frac{\hbar\omega_p}{t} > \frac{\pi B^2\varepsilon_d}{4(1 - \varepsilon_d\chi_d)}, \quad (7)$$

where  $\omega_p$  is the frequency of the Peierls mode  $\delta$ . A similar inequality follows from requiring  $\delta(B)$  to be less than the zero-point amplitude of the Peierls mode. A BOW system that satisfies Eq. (7) will appear to be regular. The inequality is for a harmonic lattice with  $\varepsilon_d\chi_d < 1$ . Related inequalities are expected for other potentials, since discernible dimerization requires a double well with finite depth.

## 3. Experimental

### 3.1. Preparation of Rb–TCNQ(II)

RbI (200 mg, 0.94 mmol) was dissolved in acetonitrile (30 mL) with heating. Similarly, TCNQ (200 mg, 0.98 mmol) was dissolved in a mixture of chloroform (20 mL) and acetonitrile (10 mL) with heating. After both solutions cooled to room temperature, the TCNQ solution was decanted into a 25 mm × 200 mm screw-capped tube (precipitated TCNQ was left behind). Acetonitrile (3 mL) was carefully layered on top of the TCNQ solution, followed by the RbI solution. The tube was capped and allowed to stand for one week in the dark, yielding numerous dark needles. The mother liquor was carefully decanted, and the remaining crystals were allowed to dry. Powder X-ray analysis showed this material to be mainly (or even exclusively) Rb–TCNQ(II), with the chief impurity Rb–TCNQ(I). For the measurements performed in this study, the crystals were separated under a microscope (due to their difference in color). The experience of several crystallization experiments showed that the best quality material is obtained from undisturbed solutions. Furthermore, at the end of the crystallization, the mother liquor must be removed very carefully, because agitation of the mixture results in the rapid crystallization of large numbers of small crystals of the undesired Rb–TCNQ(I).

### 3.2. X-ray structures of Rb–TCNQ(II)

#### 3.2.1. Summary

Two previous determinations of the structure of Rb–TCNQ(II) at room temperature have been reported [16,25]. In the present work, the structure of Rb–TCNQ(II) was determined at both 100 K and 295 K. All determinations reveal a structure in the triclinic space group  $P\bar{1}$  (No. 2) with  $Z = 1$ . Thus the TCNQ<sup>−</sup> lies on a crystallographic center of inversion, and only half of the atoms are crystallographically independent. In addition, the cell contents and

**Table 1**  
Unit cell parameters of Rb–TCNQ(II).

<i>a</i>	<i>b</i>	<i>c</i>	$\alpha$	$\beta$	$\gamma$	
9.914(1)	7.196(3)	3.930(2)	92.7(1)	86.2(1)	97.73(7)	Ref. [16]
9.907(2)	7.180(2)	3.886(1)	88.55(2)	86.86(2)	94.41(2)	Ref. [25]
9.9056(1)	7.1770(1)	3.8871(1)	88.615(1)	86.800(1)	97.417(1)	295 K
9.8173(2)	7.1482(2)	3.8310(1)	88.701(2)	85.788(2)	97.260(1)	100 K

crystal symmetry demand that the TCNQ<sup>−</sup> as well as the Rb<sup>+</sup> be evenly spaced, not dimerized. As seen in Table 1, the unit cell parameters for the four determinations are quite similar.

### 3.2.2. Detailed description

A small crystal (0.02 mm × 0.10 mm × 0.20 mm) of Rb–TCNQ(II) was employed for data collection using Mo K $\alpha$  radiation ( $\lambda = 0.71073 \text{ \AA}$ ) at 100 K. As noted by Kobayashi [25], all Rb–TCNQ(II) crystals appear to be twinned or multiple, and indeed, in the present work the intensity data were initially processed to yield a two-component non-merohedral twin data set. Further data reduction in SHELXTL yielded 3671 unique reflections ( $\theta_{\max} = 30.03^\circ$ ) that were used for the refinement. The coordinates from Ref. [25] were employed for the initial solution, and the structure was refined by full matrix least squares on  $F^2$  (SHELXTL). All atomic coordinates were refined; the non-hydrogen atoms were refined with anisotropic displacement coefficients, and hydrogen atoms were refined isotropically. The refinement converged to  $R(F) = 0.0245$ ,  $wR(F^2) = 0.0551$ , and  $S = 1.047$  for 3701 reflections with  $I > 2\sigma(I)$ , and  $R(F) = 0.0256$ ,  $wR(F^2) = 0.0557$ , and  $S = 1.048$  for 3761 unique reflections, 88 parameters, and 0 restraints. The maximum  $\Delta\sigma$  in the final cycle of least squares was less than 0.001, and the residual peaks on the final  $\Delta\rho$  map ranged from  $-0.44$  to  $0.40 \text{ e/\AA}^3$ .

The structure of Rb–TCNQ(II) at 100 K is shown in Fig. 1. The very small thermal ellipsoids (drawn at the 50% probability level), in addition to the low  $R$ -factors for the refinement, indicate that the structure is well ordered and well determined. The interplanar separation,  $R = 3.174 \text{ \AA}$ , is among the shortest in TCNQ salts [25,11]. While it is not possible to exclude dimerization entirely, the thermal ellipsoids of the quinoid atoms set a conservative upper bound of  $R_+ - R_- < 0.05 \text{ \AA}$ . Notably, the ellipsoids of the four C atoms along the central axis of TCNQ (which cannot ‘wobble’) are small and nearly spherical.

Using the same crystal, a second data set was collected at 295 K. Data reduction gave a two-component twin data set containing 3084 unique reflections ( $\theta_{\max} = 30.02^\circ$ ) that were used for the refinement. The refinement was carried out as described for the 100 K structure. It converged to  $R(F) = 0.0288$ ,  $wR(F^2) = 0.0651$ , and  $S = 1.041$  for 2899 reflections with  $I > 2\sigma(I)$ , and  $R(F) = 0.0339$ ,  $wR(F^2) = 0.0673$ , and  $S = 1.043$  for 3084 unique reflections, 88 parameters, and 0 restraints. The maximum  $\Delta\sigma$  in the final cycle of least squares was less than 0.001, and the residual peaks on the final  $\Delta\rho$  map ranged from  $-0.36$  to  $0.78 \text{ e/\AA}^3$ . The interplanar  $R$  increases to  $3.241 \text{ \AA}$  at 295 K, in agreement with  $3.25 \text{ \AA}$  reported in Ref. [25]. Crystallographic data (excluding structure factors) for these two structures have been deposited with the Cambridge Crystallographic Data Centre publication numbers CCDC 719948 and 719949.

### 3.3. Molar paramagnetic susceptibility

Magnetization measurements were done in a Quantum Design SQUID Magnetic Properties Measurement System. A total of 9.1 mg of Rb(II) was loaded in a sample holder and measured in an applied field of  $H = 10\,000 \text{ Oe}$ . The only correction applied in Fig. 2 was to subtract a temperature independent  $\chi_0$  term of  $-3.661 \times 10^{-4} \text{ emu/mol}$  to account for the sample holder and the core diamagnetism of the sample. The inset shows the raw data and a small Curie tail ( $1/T$ ) at  $T < 50 \text{ K}$ .

Our  $\chi(T)$  is consistent with that reported in Ref. [10] using electron paramagnetic resonance (epr) intensity. The knee around 220 K was taken as  $T_d$ . The Na and K–TCNQ salts, which are dimerized at 300 K, have a similar but sharper knee [10] at higher  $T_d$ . A singlet–triplet gap rationalizes an activated  $\chi(T)$  below  $T_d$ , although not quantitatively. The  $\chi(T)$  curve for  $T > T_d$  is unexpected [6] in 1D Hubbard models with regular stacks, and this unexplained behavior is common to alkali–TCNQ salts. No modeling is

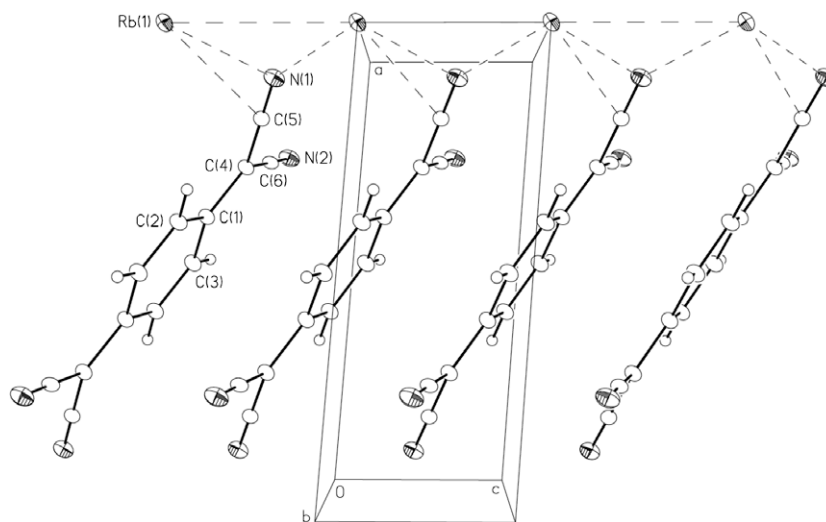


**Fig. 1.** Rb–TCNQ(II) stack at 100 K with thermal ellipsoids at the 50% probability level.

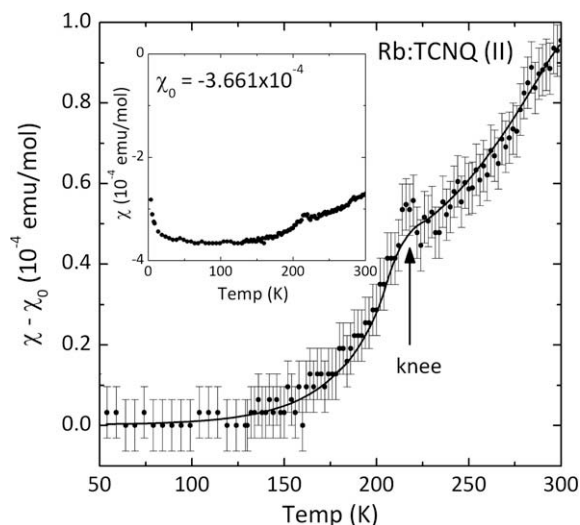


Fig. 2. Absolute molar paramagnetic susceptibility of Rb-TCNQ(II). The line is to guide the eye. The temperature independent correction is  $\chi_0 = -3.661 \times 10^{-4}$  emu/mol.

required, however, to infer that negligible  $\chi$  below 150 K indicates a singlet gs and a substantial gap  $E_m > 400$  K.

### 3.4. Infrared spectra

Totally symmetric (ts) molecular vibrations  $\omega_n$  are red shifted due to coupling to charge fluctuations along the stack [26,19]. The ir intensity  $I_n(T)$  at  $\omega_n$  vanishes by symmetry in regular stacks since modulation of  $\omega_n$  generates equal electronic fluxes to the right and left. Dimerization breaks  $C_i$  symmetry and gives strong intensity at  $\omega_n$  in parallel polarization. Powder Rb-TCNQ(II) data in Fig. 2 of Ref. [18] for  $\omega_n = 722$   $\text{cm}^{-1}$  showed a cooperative increase of  $I_n(T)$  on cooling with a point of inflection around 220 K that was interpreted [18] as  $T_d$  in view of the  $\chi(T)$  knee. We verified similar  $I_n(T)$  for three ts vibrations with  $\omega_n$  between 1100 and 1600  $\text{cm}^{-1}$  in single crystals and confirmed their polarization along the stack. Improved data collection is needed for spectra with perpendicular polarization, and both polarizations are required for a full analysis. The four coupled ts frequencies  $\omega_n > 1100$   $\text{cm}^{-1}$  of Rb-TCNQ(II) are nearly the same as in crystalline [27] K-TCNQ or in powder [28] Rb-TCNQ(I), both dimerized at 300 K. As in the case of  $\chi(T)$ , preliminary ir data are consistent with previous measurements.

## 4. Discussion

Rb-TCNQ(II) crystals at 100 K combine regular  $A^-$  stacks with magnetic and ir data that are characteristic of dimerized stacks. Small ( $<0.05$  Å) dimerization cannot be excluded without additional measurements, but that is far smaller than in Na or K-TCNQ (see below) leading to similar magnetism and ir. We again note that a dimerized half-filled stack has broken  $C_i$  symmetry and finite  $E_m$  for any degree of correlation, from bands to spin chains. The magnitude of  $E_m$ , the ir intensities and red shifts, the optical CT transition and other data require microscopic models with parameters such as  $t$ ,  $U$ , Coulomb interactions, e-ph coupling and, in some cases, 3D contributions. The BOW phase provides an alternative way to break electronic  $C_i$  symmetry and have finite  $E_m$  in half-filled Hubbard models near the CDW transition. We showed previously that 1:1 alkali-TCNQ salts are close to the CDW transition [6]. The  $P\bar{1}$  structure at 100 K, in which TCNQ $^-$  is found to lie

on an inversion center, leads us to conclude that Rb-TCNQ(II) is a realization of a BOW phase.

Dimerized, trimerized and tetramerized stacks, including many TCNQ salts, were among the first to be studied and modeled [29,7]. Epr indicates mobile triplet spin excitons with resolved fine structure confined to 1D stacks, a thermally activated concentration of triplets, and triplet-triplet collisions that result in an exchange-narrowed line with increasing  $T$ . Dimerization imposes a nondegenerate gs with  $B = p_+ - p_- > 0$  in Eq. (3). The amplitude  $B$  can be computed in models or estimated in organic crystals or conjugated polymers. Interplanar  $R_{\pm}$  between TCNQ $^-$  neighbors is the simplest measure of dimerization. Representative [11–17] values for K or Na or Rb-TCNQ(I) are  $(R_+ - R_-) \sim 0.3$  Å and  $(R_+ + R_-) \sim 6.7$  Å; their structural dimerization is  $0.3/6.7 \sim 4\%$ . Since cations also dimerize at  $T_d$ , the transition has 3D character.

The BOW phase of a regular stack with zero-point vibrations about  $\delta = 0$  has an amplitude  $B$  that switches between  $|\psi(B, \delta)|$  and  $|\psi(-B, \delta)|$ . The modulation is slow because the Peierls mode is a lattice phonon. Since ts modes above 1000  $\text{cm}^{-1}$  have an order of magnitude higher frequency, the first approximation is a frozen lattice with equal probability for  $\delta > 0$  or  $\delta < 0$ . Previous analysis can then be used for the BOW phase with broken  $C_i$  symmetry, with  $B$  estimated by comparison with dimerized stacks. Powder ir of Rb-TCNQ(II) and (I) at 300 K show [28] somewhat ( $\sim 50\%$ ) greater  $I_n$  for the dimerized form (I). The 300 K reflection spectrum of Rb-TCNQ(II) in Fig. 2b of Ref. [30] was obtained in connection with ultrafast pump-probe experiments. Similar to our results, there are four ts vibrations [30] with parallel polarization and  $\omega > 1000$   $\text{cm}^{-1}$ . Their intensity is 30–50% less than the corresponding K-TCNQ vibrations. There are important differences as well, such as the strong  $T$  dependence of  $I_n(T)$  and hence of  $B(T)$ . Either thermal excitations or modulation of the Peierls mode may rationalize  $B(T)$ .

The requirements for  $\epsilon_d \chi_d < 1$  and small  $B$  in Eq. (7) make it possible in principle for related systems to dimerize on cooling or not. Rb-TCNQ(II) has  $R = 3.241$  Å at 295 K, significantly shorter than  $R = 3.385$  Å or 3.479 Å in the regular phase [11] of Na or K-TCNQ, respectively. Small  $R$  suggests a stiff lattice with large  $\kappa$ . As noted in Section 2, the Rb(II) stacking leads to smaller  $\alpha$  than in Na or K stacks. Small  $\epsilon_d = \alpha^2/\kappa$  in Rb-TCNQ(II) favors a regular stack in Eq. (7). The Peierls mode softens as  $\epsilon_d$  in Eq. (6). Diffuse X-ray scattering in Na and K-TCNQ shows [31] a soft mode at  $T > T_d$ . A ts stretch in the CN region remains ir active above  $T_d = 395$  K in the polarized reflectance spectrum of K-TCNQ [32]. Its anomalous behavior was tentatively attributed to fluctuations in regular stacks [32], before the proposal of BOW phase [1]. Such evidence is less decisive, since the  $\chi(T)$  at  $T > T_d$  indicates spin excitations from the gs. A BOW phase offers new opportunities to account for previous  $T > T_d$  observations on alkali-TCNQ salts.

We noted at the beginning that rigorous BOW results are presently limited to 0 K. Alkali-TCNQ salts (1:1) satisfy the electrostatic requirement that a BOW phase be close to the CDW boundary. With the analysis of dimerization, we can understand the  $P\bar{1}$  structure at 100 K, finite  $E_m$  and ir intensities of Rb-TCNQ(II) as the realization of a BOW phase. Remarkably, the BOW phase of the EHM addresses precisely the Rb-TCNQ(II) conflicts that are raised most sharply by the 100 K structure and ir or  $\chi$  data. We also recognize that actual modeling rather than symmetry arguments will be needed for the magnetic, ir, optical and other properties of the alkali-TCNQ family.

### Acknowledgements

ZGS thanks A. Girlando for access to ir data prior to publication, A. Painelli for discussions about the BOW phase and the reviewer for comments about Peierls transitions. TMM gratefully acknowl-

edges support of the National Science Foundation graduate research fellowship program. This work was supported in part by NSF Grants CHE-0614879 (to RAP) and DMR-0819860 (to RJC).

## References

- [1] M. Nakamura, *Phys. Rev. B* 61 (2000) 16377.
- [2] P. Sengupta, A.W. Sandvik, D.K. Campbell, *Phys. Rev. B* 65 (2002) 155113.
- [3] Y.Z. Zhang, *Phys. Rev. Lett.* 92 (2004) 246404.
- [4] S. Glocke, A. Klumper, J. Sirker, *Phys. Rev. B* 76 (2007) 155121.
- [5] M. Kumar, S. Ramasesha, Z.G. Soos, *Phys. Rev. B* 79 (2009) 035102.
- [6] M. Kumar, S. Ramasesha, Z.G. Soos, *Eur. Phys. Lett.* 83 (2008) 37001.
- [7] Z.G. Soos, *Ann. Rev. Phys. Chem.* 25 (1974) 121.
- [8] Z.G. Soos, D.J. Klein, in: N.B. Hannay (Ed.), *Treatise on Solid State Chemistry*, vol. III, Plenum, New York, 1976, p. 689.
- [9] J.S. Miller (Ed.), *Extended Linear Chain Compounds*, vol. 3, Plenum, New York, 1983.
- [10] J.G. Vegter, J. Kommandeur, *Mol. Cryst. Liq. Cryst.* 30 (1975) 11.
- [11] H. Endres, in: J.S. Miller (Ed.), *Extended Linear Chain Compounds*, vol. 3, Plenum, New York, 1983, p. 263.
- [12] M. Konno, Y. Saito, *Acta Cryst. B* 30 (1974) 1294.
- [13] M. Konno, Y. Saito, *Acta Cryst. B* 31 (1975) 2007.
- [14] M. Konno, T. Ishii, Y. Saito, *Acta Cryst. B* 33 (1977) 763.
- [15] A. Hoekstra, T. Spoelder, A. Vos, *Acta Cryst. B* 28 (1972) 14.
- [16] I. Shiratoni, H. Kobayashi, *Bull. Chem. Soc. Jpn.* 46 (1973) 2595.
- [17] B. van Bodegom, J.L. de Boer, A. Vos, *Acta Cryst. B* 33 (1977) 602.
- [18] R. Bozio, C. Pecile, *J. Chem. Phys.* 67 (1977) 3864.
- [19] R. Bozio, C. Pecile, in: R.J.H. Clark, R.E. Hester (Eds.), *Spectroscopy of Advanced Materials*, *Adv. Spectrosc.*, vol. 19, Wiley, New York, 1991, p. 1.
- [20] A.J. Heeger, S. Kivelson, J.R. Schrieffer, W.P. Su, *Rev. Mod. Phys.* 60 (1988) 81.
- [21] W.P. Su, J.R. Schrieffer, A.J. Heeger, *Phys. Rev. B* 22 (1980) 2099.
- [22] P. Sengupta, A.W. Sandvik, D.K. Campbell, *Phys. Rev. B* 67 (2003) 245103.
- [23] J. Huang, M. Kertesz, *Chem. Phys. Lett.* 390 (2004) 110.
- [24] Z.G. Soos, D. Mukhopadhyay, A. Painelli, A. Girlando, in: T.A. Skotheim, R. Elsenbaumer, T. Allen (Eds.), *Handbook of Conducting Polymers*, Sec. Edit., Marcel Dekker, New York, 1997, p. 165.
- [25] H. Kobayashi, *Bull. Chem. Soc. Jpn.* 54 (1981) 3669.
- [26] A. Girlando, A. Painelli, S.A. Bewick, Z.G. Soos, *Synth. Met.* 141 (2004) 129.
- [27] D.B. Tanner, C.S. Jacobsen, A.A. Bright, A.J. Heeger, *Phys. Rev. B* 15 (1977) 3283.
- [28] R. Bozio, I. Zanon, A. Girlando, C. Pecile, *J. Chem. Soc., Faraday Trans.* 274 (1978) 235.
- [29] P.L. Nordio, Z.G. Soos, H.M. McConnell, *Ann. Rev. Phys. Chem.* 17 (1966) 237.
- [30] K. Ikegami et al., *Phys. Rev. B* 76 (2007) 085106.
- [31] H. Terauchi, *Phys. Rev. B* 17 (1978) 2446.
- [32] H. Okamoto, Y. Tokura, T. Koda, *Phys. Rev. B* 36 (1987) 3858.